JJEES

JJEES (2025) 16 (4): 418-432
ISSN 1995-6681

Jordan Journal of Earth and Environmental Sciences

Spatiotemporal Analysis of Wetland Environmental Changes Using Machine Learning and Remote Sensing Data

Yulia Fitriani, Nurlina Abdullah* , Ichsan Ridwan

Geophysics, Faculty of Mathematics and Natural Sciences, Universitas Lambung Mangkurat, Banjarbaru, Kalimantan Selatan, Indonesia

Received on March 23, 2025, Accepted on June 5, 2025

Abstract

Wetlands are essential ecosystems that provide vital services but are vulnerable to degradation. Hulu Sungai Utara (HSU)) Regency, South Kalimantan, hosts extensive tropical peatland wetlands spanning over 64,821 hectares. These wetlands are significant but face considerable shrinkage due to reduced water flow and land conversion. This study examined spatiotemporal changes in wetland cover in HSU from 2000 to 2024 using Landsat 7 ETM+ and Landsat 8 OLI data on Google Earth Engine (GEE). We used NDWI, NDVI, and MNDWI indices along with Machine Learning algorithms—Random Forest (RF) and Support Vector Machine (SVM)—for classification into water, vegetation, built-up, and barren land. RF achieved higher accuracy (97.33% overall accuracy, 96% average kappa), effectively mapping transitions. Results reveal a long-term decline in wetlands (loss of 71.4 km²), driven by development, climate change, and human activity. Notably, a significant regeneration trend appeared over the past 15 years, with gains exceeding losses in this recent period. This highlights the potential of GEE-based geospatial technology for data-driven tropical wetland conservation, suggesting positive effects from recent initiatives.

Keywords: *Wetland Water Index; Machine Learning; Google Earth Engine; Land Cover*

1. Introduction

A wetland is an environment where land meets water, often partially adjacent to a body of water. These systems can contribute significantly to the surrounding environment, including being important to unique species of plants and animals that live there (Mahdavi et al., 2018). A wetland is a rich source of food, raw materials, and water resources for people. The area also strengthens water sources, replenishes groundwater, and controls soil erosion. For this reason, wetland is called "Kidney of the Earth" (Zhang et al., 2023). A wetland is an area that contains water, has hydric soils, and supports certain vegetation that is adapted to wet environments. Additionally, the land is also waterlogged during certain seasons of the year (Mirmazloumi et al., 2021). Over the last few decades, wetlands in tropical countries such as Indonesia have experienced severe degradation. This decline is attributed to several factors, including population growth, infrastructure development, pollution, resource overexploitation, climate change, and poor governance. The facts show the importance of wetland risk assessment and monitoring using modern geospatial technologies and analytical methods (Aslam et al., 2024).

Remote sensing (RS), combined with wetland science, is being used more effectively than ever to accurately measure wetland quality and changes over time. Wetland mapping using Earth observation data captures information about the Earth's surface at low to very high resolution (Awawdeh et al., 2023). Additionally, the application of earth observation data is essential for managing natural resources at the regional, national, and international levels. Wetland monitoring is challenging, specifically at large scales, due to the diverse and fragmented wetland ecosystems and the spectral similarities among different wetland types (Abdelmajeed et al., 2023). To collect wetland cover information from Landsat, the image will be categorized, tagged, and entered into a GIS to undergo the the image interpretation process. Moreover, the spatiotemporal dynamics of the Hulu Sungai Utara Regency wetland in South Kalimantan are monitored using remote sensing images at a the spatiotemporal scale (Wu et al., 2020; Nurlina et al., 2024). Actual annual wetland areas can be mapped at the regional level using multitemporal Landsat 8-OLI and 7-ETM+ water change data collected from 2000 to 2024. This process is performed using several satellite-derived applications for land cover, including the Normalized Difference Water Index (NDWI), Normalized Difference Vegetation Index (NDVI), and Modified Normalized Difference Water Index (MNDWI) (Ashok et al., 2021).

NDVI in wetland mapping is utilized for drought monitoring, assessing plant cover, monitoring vegetation, and evaluating agricultural drought. However, remote sensing tools operating in near-infrared (NIR), shortwave infrared (SWIR), and thermal infrared (TIR) bands can identify water stress (Shashikant et al., 2021). Non-dimensional index known as NDVI uses the difference between visible and NIR reflectance to determine vegetation cover. A frequently used index to track vegetation dynamics at regional and global levels is NDVI. Following this discussion, vegetation density is estimated using NDVI measurements (Ashok et al., 2021). Using NDWI allows monitoring of vegetation

* Corresponding author e-mail: nurlina_abdullah@ulm.ac.id

moisture content by focusing on a specific area of the spectrum. This index is often applied to check the evaluation of drought conditions through the analysis of vegetation (Shashikant et al., 2021). Landsat TM Bands 2 and 4 are used to extract water features for NDWI. The index uses two improved Random Forest (RF) classifiers with Landsat 8 OLI to classify possible water bodies (Ichsan Ali et al., 2019). MNDWI is used to define landscape patterns, water bodies, and ecological study. Therefore, to assess how drainage systems and flooded areas have changed over the past decades. Drainage system studies and MNDWI analysis are used to find the upward trend in flooded areas over a predetermined period (Rashid, 2023).

Machine learning is a practical method for simulating complex ecological events using multivariate geographic data. Algorithms such as Support Vector Machine (SVM), RF, and artificial neural networks have been highly effective in mapping wetlands and detecting change across various areas globally. This model enables the forecasting of wetland hazards in the context of potential future environmental changes, utilizing RF categorization on Google Earth Engine (GEE) and Landsat image collections. GEE is a cloud platform for viewing, computing, and analyzing planetary-scale satellite imagery. This platform has been utilized in numerous studies, including land cover analysis, urban expansion, vegetation change, and disaster monitoring, as well as wetland change (Yan et al., 2022). The main focus of GEE is to develop highly interactive online algorithms, applying big data analysis expertise to remote sensing with a significant impact that enables data-driven science based on global challenges, including large geospatial datasets. Moreover, the platform deliverables are designed to analyze and store vast datasets at the petabyte level (Ashok et al., 2021).

Prior studies have demonstrated the efficacy of remote sensing and machine learning techniques for wetland monitoring and change detection in various regions globally and within Indonesia (Long et al., 2021; Waleed et al., 2023). Previous research utilized time series remote sensing data and the extreme gradient boosting (XGBoost) method to generate land use maps of the Yellow River Delta (YRD) in China from 2000 to 2020 (Zhu et al., 2024). This method proved to be effective, with land use classification achieving an accuracy of 90.45% based on Landsat time series data and the XGB method. Other research explored the use of ten machine learning algorithms available on Google Earth Engine (GEE) for multi-temporal land use mapping in the Segara Anakan coastal wetland area, using Landsat imagery from 1978, 1991, 2001, and 2014. The results show that the CART (Classification and Regression Tree) algorithm achieved the highest accuracy of 96.98% (Overall Accuracy) using K-Fold Cross Validation (K=10), demonstrating the effectiveness of GEE and machine learning for multi-temporal land use mapping (Farda, 2017).

However, a comprehensive spatiotemporal analysis focusing specifically on the extensive and vulnerable tropical peatland wetlands of Hulu Sungai Utara Regency, South Kalimantan, using a combined approach of multiple spectral indices (NDVI, NDWI, MNDWI) and advanced machine learning classifiers (Random Forest and Support Vector Machine) over a long-term period (2000-2024) implemented on the Google Earth Engine platform has not been previously conducted. This research fills a critical gap by providing a detailed, multi-decadal assessment of wetland dynamics in this ecologically significant area, leveraging the computational power of GEE to process large volumes of Landsat data and offering novel insights into the patterns and drivers of change, including the identification of recent regeneration trends. The main objective is to develop and analyze various Landsat 7 and 8 time series methods to map wet areas using GEE. Based on NDVI, NDWI, and MNDWI, the proposed algorithm can accurately record changes in wetland cover. This study examines the spatial and temporal changes of a selected wetland from 2000 to 2024, both quantitatively and qualitatively. The results can serve as the basis for a deeper understanding of how thewetland regime has changed over the years. The objectives include (i) Evaluating wetland areas based on Landsat images based on NDVI, NDWI, and MNDWI, (ii) Identifying the presence of permanent water bodies during the 5-year interval from 2000 to 2024, (iii) Performing image classification using guided classification RF and SVM.

2. Methodology

2.1 Study Area

The study area was located in the Peat Hydrology Unit (PHU), Hulu Sungai Utara Regency, South Kalimantan Province, Indonesia. Wetland cover in this area had an area of 648 km^2 with coordinates 2^o 26'26.81 "S 115^o 11'12.44" E (Figure 1), which was a wetland in South Kalimantan where most of the soil was peat and swamp land. Following the description, the area was located about 79 km from Banjarbaru City.

The primary issue with this wetland was the gradual reduction in size resulting from changes in sedimentation and infrastructure development. Therefore, this study aimed to understand the intensity of wetland cover change, focusing on the temporal and spatial changes of Hulu Sungai Utara Regency wetlands between 2000 and 2024 using histograms of surface water events. Understanding the relevance of water levels at the study site during this time was aided by an examination of worldwide surface water events and seasonal water changes, facilitated by an analysis of global surface water events and seasonal water fluctuations.

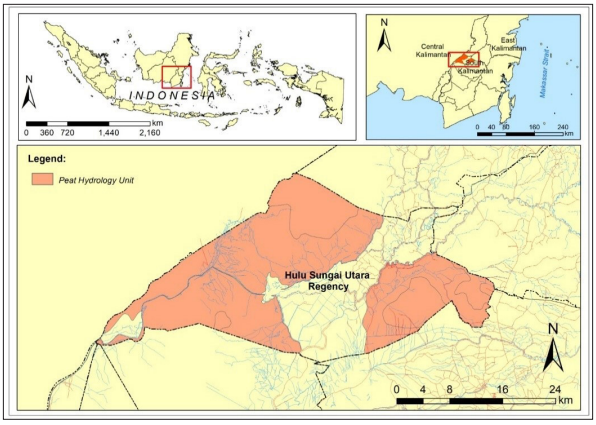

Figure 1. Map of the Study Area at Hulu Sungai Utara Regency, Indonesia

2.2 Data Collection

Multi-temporal satellite imagery was acquired to record changes in Hulu Sungai Utara Regency over the past 24 years, from 2000 to 2024. Landsat 7 ETM+ and 8 (OLI) missions provided this imagery, which had a temporal frequency of 16 days and a spatial resolution of 30 m. Specifically, Landsat 7 Enhanced Thematic Mapper Plus (ETM+) data for the years 2000 to 2010, and Landsat 8 Operational Land Imager (OLI) data for 2015-2024 were used (Aslam et al., 2024). NDVI, NDWI, and MNDWI time series from 2000 to 2024 were calibrated using 5-year gaps, utilizing Landsat 7 and 8 Collection 2 Tier 1 Raw Scenes. Table 1 shows the details of Bands 1 to 7 with their original spatial resolution using GEE. This platform included Landsat-specific processing methods to calculate sensor radiance, TOA reflectance, surface reflectance (SR), cloud score, and cloud-free composite. GEE also provided an algorithm to create a simple composite of the Landsat image, namely ee.Algorithms.Landsat. simple Composite(). The algorithm combined composites of multiple Landsat images to produce a clean image by minimizing the effects of disturbances such as clouds and cloud shadows. Moreover, cloud computing technology was used in this platform to process Landsat data (https://earthengine.google.org/). This process enabled parallel computing and processing of large data in the study area.

Table 1. Landsat data description

ID	Description
LANDSAT/LE07/C02/T1	Landsat 7, Collection 2, Tier 1 Raw Scenes
LANDSAT/LC08/C02/T1	Landsat 8, Collection 2, Tier 1 Raw Scenes

2.3 Spectral Water Index Calculation

NDVI has been widely used to analyze changes in vegetation cover over time and space (Andini et al., 2024). By applying the Red and NIR bands, the vegetation index determines the balance between energy absorbed and released by Earth objects (Hashim et al., 2019). In addition, NDVI was calculated based on the surface reflectance bands of 7 and 8 in the following Equation.

$$NDVI = \frac{(NIR-RED)}{(NIR+RED)} \quad (1)$$

Where NIR and RED represented the reflectance of bands 4 & 3 on Landsat 7 and bands 5 & 4 on Landsat 8, respectively. Following this discussion, vegetation changed over time with the application of atmospheric correction.

NDWI is used in Landsat image analysis to identify open water features using NIR and visible green (GREEN) spectral bands (Laonamsai et al., 2023). The model value was a useful indicator of plant water stress because it was closely related to the moisture content of plants sensitive to built-up land. This study primarily focused on the reflectance characteristics of dry and green vegetation. During the analysis, water bodies were extracted from a satellite image using the reflectance index, which varied from -1 to +1. The surface reflectance of NIR and SWIR bands of Landsats 7 and 8 was used to calculate NDWI (Ashok et al., 2021). Additionally, the index calculated based on the surface reflectance bands of Landsat 7 and 8 was shown in the following Equation.

$$NDWI = \frac{(GREEN-NIR)}{(GREEN+NIR)} \quad (2)$$

Where GREEN and NIR represented the reflectance of band 2 & 4 on Landsat 7 and band 3 & 5 on Landsat 8, respectively.

During this study, MNDWI distinguished between non-watery and watery areas. This method used shortwave infrared 1 (SWIR1) and GREEN spectral bands (Laonamsai et al., 2023). Xu (2006) formed an algorithm that efficiently suppressed and even eliminated the effects of noise from the ground and vegetation, as well as from the water surface. Therefore, improving the final MNDWI results led to more precise data extraction from an image containing vegetation, soil, and built-up land (Sherstobitov et al., 2021). The index was calculated based on land surface reflectance bands 7 and 8 was conducted using the following Equation.

$$MNDWI = \frac{(GREEN-SWIR1)}{(GREEN+SWIR1)} \quad (3)$$

Where GREEN and SWIR1 showed the reflectance of band 2 & 5 on Landsat 7 and band 3 & 6 on Landsat 8, respectively.

A total of 648 km^2 formed a truncated geometry (the area under study) in and around Hulu Sungai Utara Regency wetland, as shown in Figure 1. Based on the difference between NDVI, NDWI, and MNDWI values, the wetland hidden in Landsats 7 and 8 images was cloud-free in late July and early August. Moreover, Landsat data had gone through an automatic cloud masking process. The selected wetland plant image depicted the plants during the budding phase, encompassing vegetative growth, reproduction, and maturation. The image was distinguished by having higher NDVI values than NDWI and MNDWI. This outcome signified that permanent water bodies had - -1 < NDVI-NDWI-MNDWI < 0, while pixels covered by vegetation had a relationship of 0 < NDVI-NDWI-MNDWI < 1. The result was used to calculate the area related to vegetation, soil, built-up areas, and water bodies in summer, specifically from late July to early August from 2000 to 2024, as indicated by the algorithm. During the analysis, a process for mapping wetland areas using GEE was proposed.

2.4 Image Classification

Class information from a multi-band raster image was extracted using image classification. Supervised classification methods, such as CART, RF, Naïve Bayes, and SVM, were applied to handle guided classification using conventional machine learning methods within the GEE framwwork. In this case, Random Forest and SVM classifiers were used from 2000 to 2024. The defined classes were divided into four classification categories, namely water, vegetation, built-up, and barren land. This process determined how RF and SVM classifiers performed.

RF was an ensemble learning method that built a large number of decision trees during training for tasks such as regression and classification. The class selected by the majority of the trees was the output of RF for classification problems. By reducing overfitting and improving prediction accuracy through feature randomness during tree splitting

and packing (bootstrap aggregating), RF outperformed single decision trees. RF was well known for its resistance to overfitting and its capacity to manage very large datasets with high dimensionality (Aslam et al., 2024).

The concepts of classification and regression were the main focus of SVM, which was an implementation of the supervised learning paradigm. SVM only classified data linearly at an early stage by creating a hyperplane. Later in 1992, Vapnik, Boser, and Guyon presented a method for forming nonlinear classifiersusing Kernel functions (Vapnik and Cortes first introduced kernels in a 1995 study paper). Following the occurrence, SVM has become a popular classification algorithm for supervised learning, i.e., datasets categorized by class labels and attributes. Unsupervised learning, or datasets without output features and class labels, was implemented using SVM clustering (Ghosh et al., 2019).

A land cover map of Hulu Sungai Utara Regency was created and assessed using Landsat 8 surface reflectance data by applying eight different combination procedures. During this process, training was conducted using MODIS land cover data from the IGBP classification. To train the sample data, both the RF classifier and SVM were used, and multiple random seeds were employed to obtain validation data. After the process, any zero pixels were removed from the results by filtration, and the data was verified based on the smiling RF. By specifying land cover category characteristics as attributes of four classes, RF classifieree. Classifier.smileRandom Forest(100).train() was applied to the training data. The output results showed that all eight datasets produced land cover maps with moderate to highly accurate accuracy with a total accuracy of more than 90%.

The Confusion Matrix and its derived accuracy index were used to evaluate the classification accuracy of each scenario data set. Each pixel in each polygon was categorized as a training point when the training dataset consisted of polygons representing homogeneous regions. Additionally, a machine learning algorithm was trained using these polygons (Stehman, 1997). The confusion matrix was a way to review how well a classification algorithm performed and provided a better understanding of the classification model and its errors. The method, sometimes referred to as an error matrix, was a quantitative method used to describe the accuracy of image classification. The matrix showed the relationship between the reference image and the classification result. The matrix requires ground-truth information, such as geographic data and the results of manual image digitization. During this study, the classification of Hulu Sungai Utara Regency wetland images was performed using GEE and Landsat 7 and 8 images. Training samples of polygon feature classes or shapefiles were provided to perform classification. In addition, the attribute table of the training samples and the format of the feature class were the same. The "Training Samples Manager" was used to build a reference dataset to ensure this process by reading and writing the dataset. A total evaluation of the classification accuracy was provided by the Kappa agreement statistic. Table 2 shows the accuracy statistic ranging from 0 to 1, with 1 signifying 100% accuracy. The overall research method is described in Figure 2.

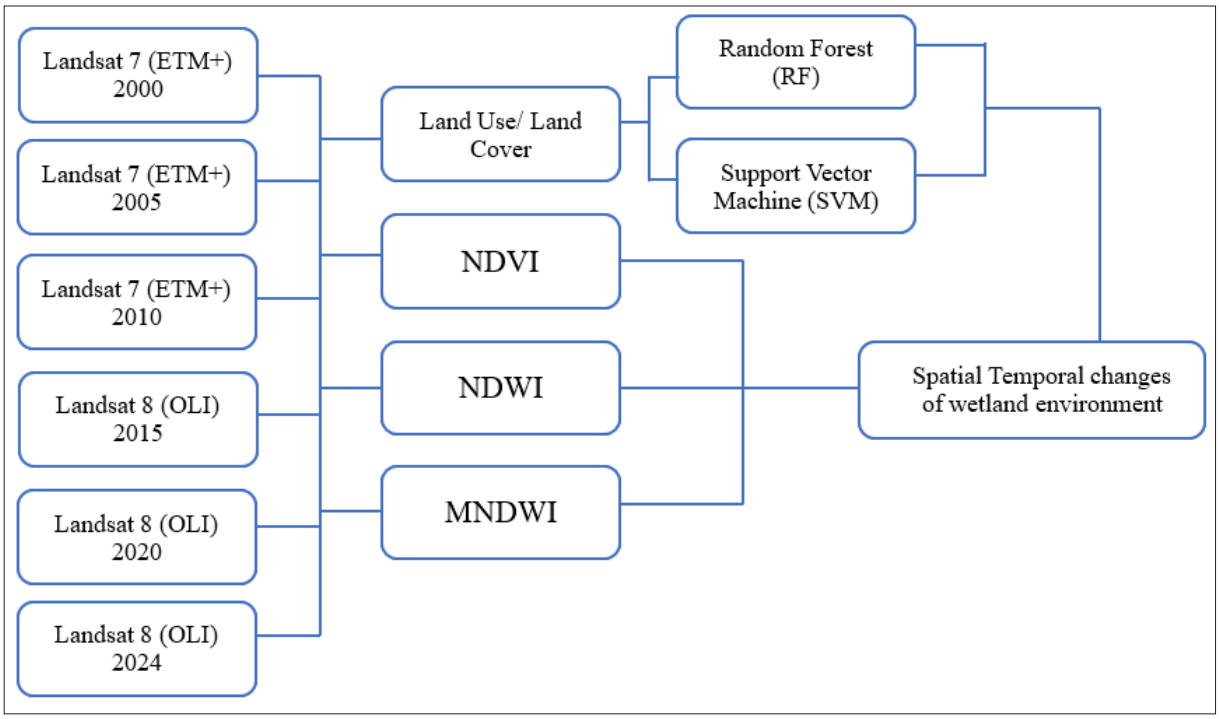

Figure 2. Study Flow Chart

3. Results and Discussion

3.1 Accuracy Assessment

Landsat image data that was classified using a Region of Interest (ROI) as a reference was applied to determine land use/cover factors. There were two types of ROI samples used, namely, testing and training samples. A testing sample was used as a representative sample for land cover classification in Google Earth, which was applied to evaluate the classification accuracy. Meanwhile, the training sample was used as a representative sample for land cover classification

(Nurlina et al., 2023). These samples were subsequently used for validation and a total accuracy test. The hue of pixels corresponding to vegetation or water bodies in the wetland was determined based on the samples. Regarding the process, JavaScript programming on the GEE platform was used to determine the areas covered by vegetation and water.

Based on Table 2, the RF model had a high average kappa accuracy of 96% and a total accuracy of 97.33% for the six years studied (2000, 2005, 2010, 2015, 2020, and 2024). An average user validation accuracy of 87.8% over 6 years showed the condition of land cover class assignment. RF showed higher classification accuracy than Support Vector Machine (SVM) in mapping wetland change. On the GEE platform, RF is efficient for large datasets as it can be parallelised, while SVM with complex kernels may be more computationally intensive. RF tends to be more robust to noise and outliers than SVM. The advantages of RF are its ability to handle complex data and its robustness, while SVM is versatile with kernels but sensitive to noise and requires careful parameter tuning (Aljanabi & Dedeoğlu, 2025; Thanh Noi & Kappas, 2017). The superior performance of RF in this study is likely due to its robustness in handling the complexity of multi-temporal data in dynamic tropical wetland environments. This outcome characterized the multitemporal variability of the wetland as well as map, and track changes over time using extended time series imagery. Landsat 7 and 8 images were used to extract the land cover shape of Hulu Sungai Utara Regency. Landsat 7 and 8 imagery spanned from 2015 to 2024, and 2000 to 2010.

Table 2. Comparison accuracy between Landsat 7 and 8 image collections over Wetland of Hulu Sungai Utara Regency (2000–2024).

Random Forest (RF)						
	Landsat 7			Landsat 8		
	Year 2000	Year 2005	Year 2010	Year 2015	Year 2020	Year 2024
Total Accuracy	0.98	0.96	0.96	0.99	0.97	0.99
Validation Accuracy	0.96	0.74	0.92	0.89	0.9	0.84
Kappa Coefficient	0.97	0.94	0.94	0.98	0.9	0.98

The main parameters in the accuracy assessment included total accuracy, i.e., the proportion of training samples that were correctly classified (70%). Other parameters included the Kappa coefficient, a measure that considered the chance of agreement. In addition, validation accuracy consisted of the proportion of training samples that were correctly classified (30 %).

3.2 Land Use and Land Cover (LULC)

Using two machine learning algorithms on GEE, RF, and SVM, land use and land cover (LULC) analysis conducted in this study revealed important changes in the distribution. The analysis also found an interesting proportion of major land cover classes surrounding the wetland in the ecologically important Hulu Sungai Utara Regency between 2000 and 2024. Following the discussion, two important physical components that measure the surface of the Earth were LULC. To distinguish between these components, a categorization system was necessary. The system provided a fundamental structuring function by offering tools to name, classify, and recognize objects on Earth (Nedd et al., 2021).

The results shown in Figure 3 were obtained from RF classification, which consisted of 4 land cover classes. Land cover classes consisted of water, vegetation, built-up, and barren land. Images from Landsat 7 and 8 were captured in the year 2000-2024, as the RF model showed higher accuracy than SVM. The results showed a decrease in the exposed and unvegetated land surface around the wetland, which was attributed to artificial reforestation initiatives in the area as well as climate change-related variables. The climate variables included increased rainfall that promoted the growth of vegetation cover (Khalaf, 2024; Aslam et al., 2024).

Machine learning based on the supervised learning model is called SVM. Statistical learning theory served as the foundation for SVM, which classified data by identifying a set of support vectors from a sample (Mohammadi et al., 2021). Moreover, the results shown in Figure 4 were divided into the same four classes as RF. The high rainfall pattern in the multitemporal analysis from 2000 to 2005 led to a slight increase in water area. The significant decrease in water area between 2005 and 2010 was offset by an increase in vegetation area. Additionally, rapid growth led to substantial changes in vegetation from 2010 and 2015. The amount of green land decreased as the number of buildings increased between 2015 and 2020. Due to urbanization around wetland, there was a reduction in water bodies in 2020-2024. Relating to this discussion, combining studies of land use and population change led to a more comprehensive knowledge of interconnected environmental as well as human factors that impacted the vulnerability of wetland in the area (Mohammadi et al., 2021).

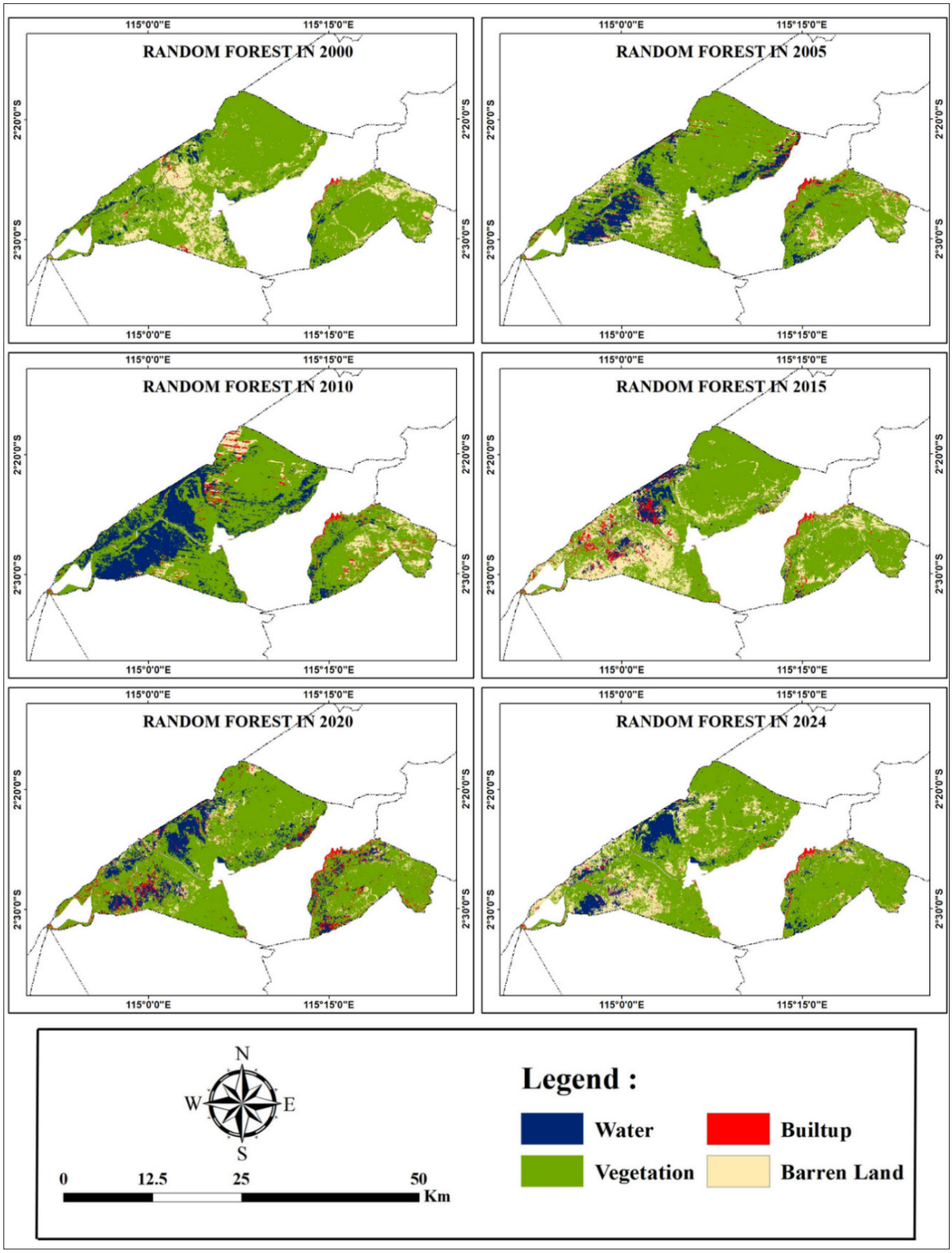

Figure 3. Land cover classification RF map from 2000 to 2024

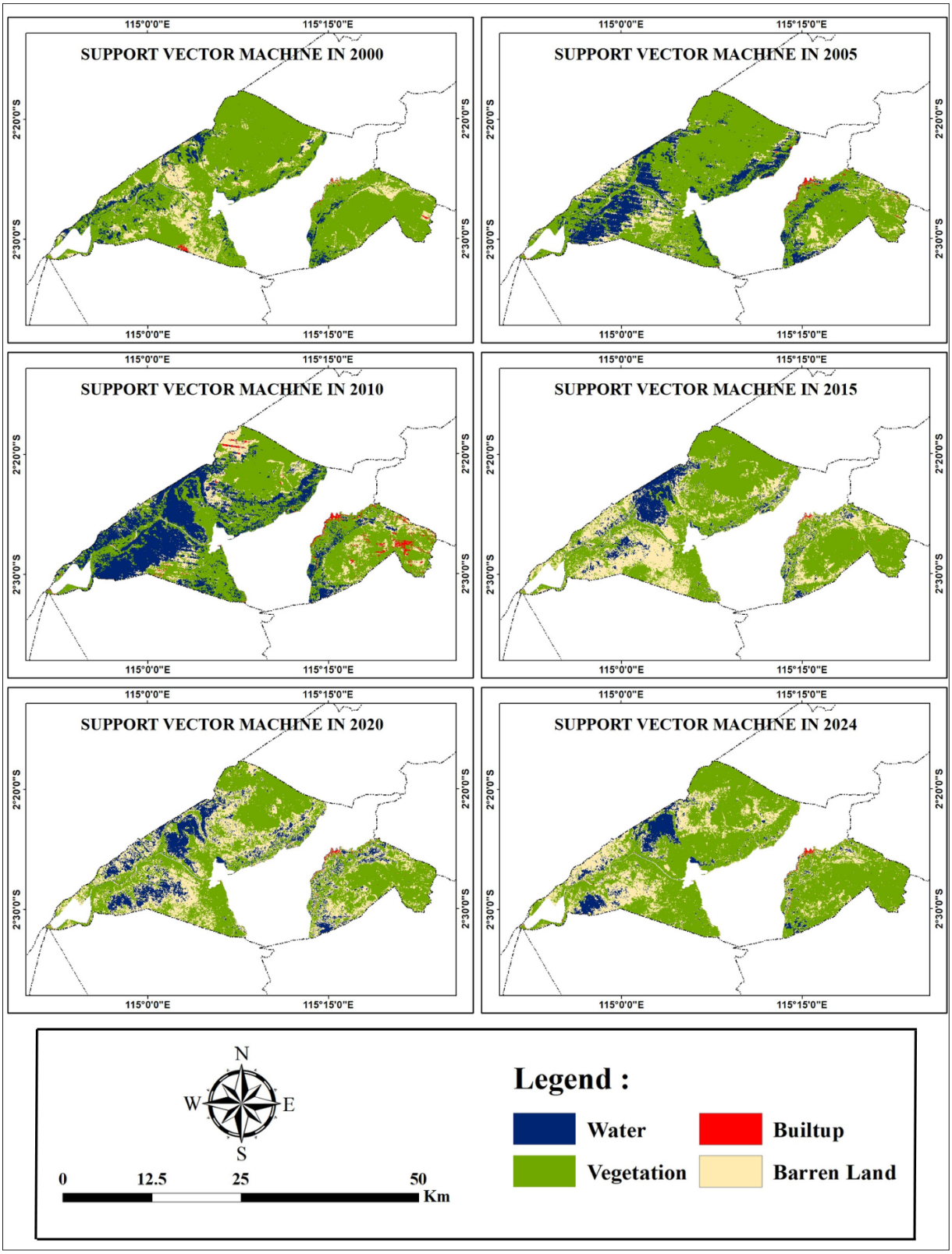

Figure 4. Land cover classification with SVM from 2000 to 2024

3.3 Transition of Wetland

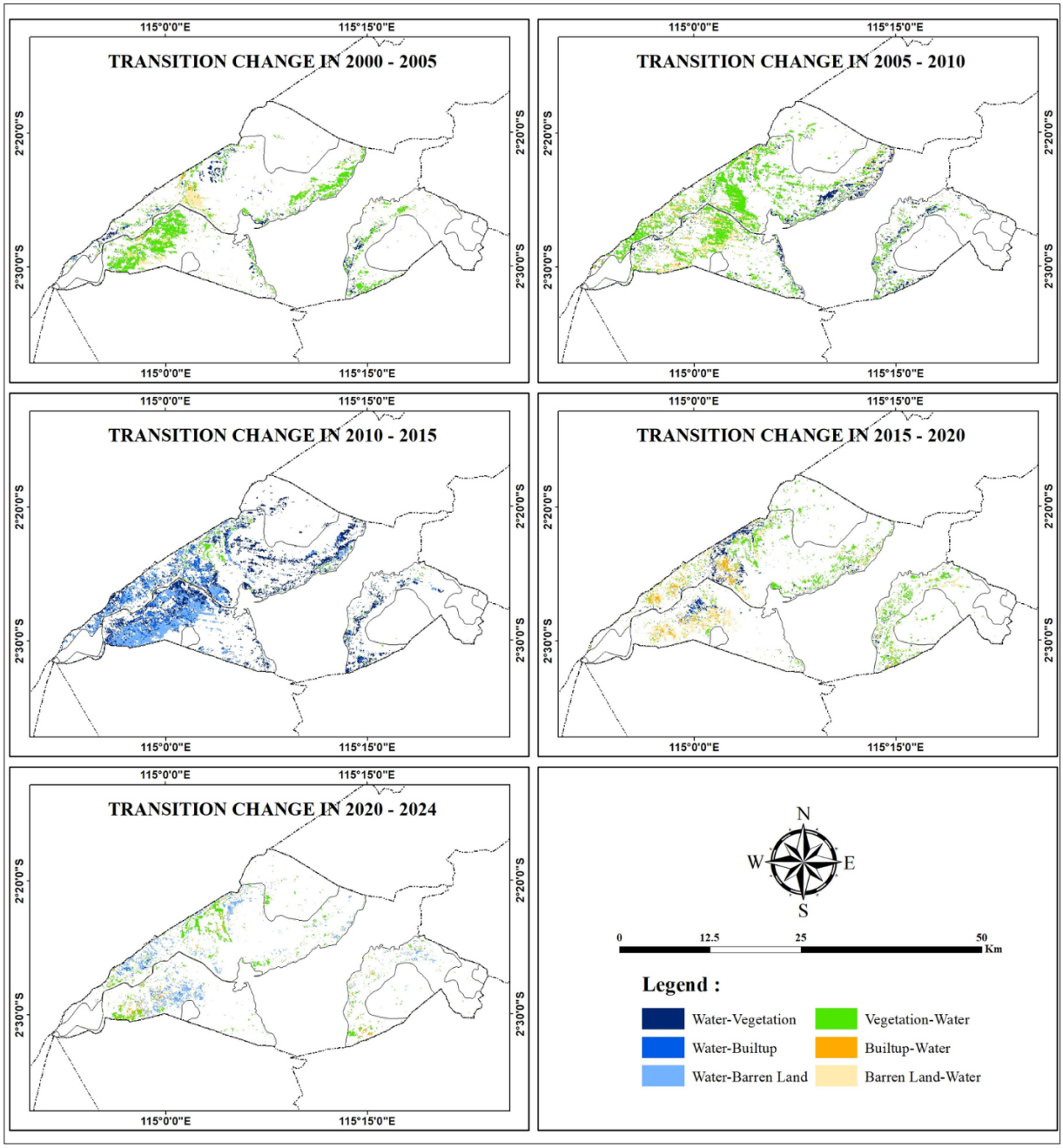

Figure 5. Transition change in wetland classes

Figure 5 presents a comprehensive wetland change detection study, which found significant transitions between wetland and other major land cover classes, such as vegetation, built-up land, and barren land, around the Hulu Sungai Utara Regency wetlands between 2000 and 2024. Specifically, during this period, 83.4 km^2 of vegetation cover and 34.7 km^2 of bare land changed to wetland. The outcome signified that wetland shrank significantly into previously unvegetated bare areas and also former forests or shrublands. This occurrence might be due to the lowered water table and low rainfall, which allowed the swamp habitat to not thrive. Consequently, 111.9 km^2 of wetland changed to vegetation cover, and 78.8 km^2 changed to bare land. Table 3 showed the conversion of a small area of 17.1 km^2 from built-up land to wetland signifying the regeneration of wetland into pavement zones that were previously built-up land. However, only 18.5 square kilometers of marsh changed to built-up land between 2000 and 2024. Table 3 showed the main transitions from bare surfaces to vegetated surfaces to wetland, signifying that wetland expansion mostly occurred on bare, non-vegetated land. Table 4 showed how the area of wetland change decreased and increased. Relating to the discussion, the area decreased as the result became negative, and it increased when the value was positive. Table 3 also measured the minimal interaction that occurred around Hulu Sungai Utara Regency between wetland and constructed impervious surfaces (DeLancey et al., 2022).

Table 3. LULC Area from 2000 to 2024

Classifier	Name	2000		2005		2010		2015		2020		2024	
	Class	km²	%	km²	%	km²	%	km²	%	km²	%	km²	%
RF	Water	21.9	3	78.3	12	161.3	25	35.7	6	90.4	14	60.7	9
	Vegetation	505.8	78	486.3	75	422.2	65	444.9	69	484.8	75	471.8	73
	Builtup	6.8	1	16.7	3	18.3	3	26.5	4	33.6	5	12.3	2
	Barren Land	113.5	18	66.7	10	46.2	7	140.9	22	39.2	6	103.3	16
	Total	648	100	648	100	648	100	648	100	648	100	648	100
SVM	Water	44.8	7	120.5	19	204.8	32	64.3	10	99.6	15	50	8
	Vegetation	509.6	79	445.3	69	347.2	54	391.8	60	332.9	51	450.2	69
	Builtup	2.6	0	3.8	1	12.6	2	1.1	0	1.9	0	1.8	0
	Barren Land	91	14	78.4	12	83.3	13	190.8	29	213.7	33	146	23
	Total	648	100	648	100	648	100	648	100	648	100	648	100

Table 4. LULC Area change from 2000 to 2024

Classifier	Name	Area Km² Change					Area % Change				
	Class	2000-2005	2005-2010	2010-2015	2015-2020	2020-2024	2000-2005	2005-2010	2010-2015	2015-2020	2020-2024
RF	Water	-56.4	-83	125.6	-54.7	29.7	-8.7	-12.8	19.4	-8.4	4.6
	Vegetation	19.5	64.1	-22.7	-39.9	13	3.0	9.9	-3.5	-6.2	2.0
	Builtup	-9.9	-1.6	-8.2	-7.1	21.3	-1.5	-0.2	-1.3	-1.1	3.3
	Barren Land	46.8	20.5	-94.7	101.7	-64.1	7.2	3.2	-14.6	15.7	-9.9
SVM	Water	-75.7	-84.3	140.5	-35.3	49.6	-11.7	-13.0	21.7	-5.4	7.7
	Vegetation	64.3	98.1	-44.6	58.9	-117.3	9.9	15.1	-6.9	9.1	-18.1
	Builtup	-1.2	-8.8	11.5	-0.8	0.1	-0.2	-1.4	1.8	-0.1	0.0
	Barren Land	12.6	-4.9	-107.5	-22.9	67.7	1.9	-0.8	-16.6	-3.5	10.4

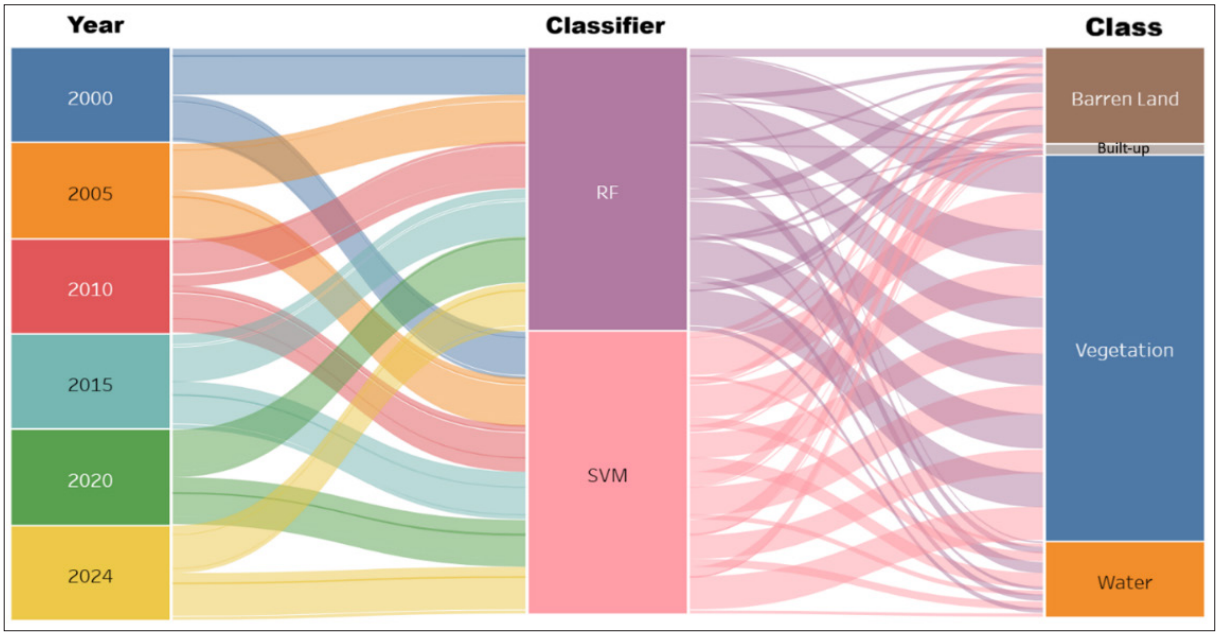

Figure 6. Trend of Land cover change from 2000 to 2024

Figure 6 shows the long-term trend from 2000 to 2024, which reveals a net decrease in wetland cover. This visually demonstrates the movement of area between the barren land, vegetation, and water classes at each time interval. While there are areas of wetlands converting to vegetation or bare land, there is also the reverse process of areas of vegetation and bare land converting to wetlands. There is a significant trend of wetland regeneration over the last 15 years (approximately 2015-2024), where the gains in wetland area outweigh the losses in this more recent period. The Sankey diagram visually supports a transition towards the ‘‘‘Water’ class in the later years (2015, 2020, 2024),

3.4 Wetland Change

According to wetland change analysis compiled in Tables 3 and 4, there was a net decrease in wetland cover over the first 15 years, as the loss of 7.7 sq. km exceeded the increase of 34.3

sq. km between 2015 and 2024. However, there was a reversal of the trend, with wetlands increasing by a total of 86.7 km², greater than the loss of 63.7 km². This reversal demonstrated that, over the last 15 years, wetland regeneration had outpaced loss, largely due to increased conservation efforts in the area. The total wetland loss of 71.4 km² for the 24 years from 2000 to 2024 was greater than the total wetland increase of 237.6 km², signifying a long-term decline. This outcome showed ecological resilience as prominent wetland ecosystems persisted despite certain losses. Although there was a late decline in wetland between 2015 and 2024, regenerative processes outpaced losses in the following 15 years. Figure 7 showed that the long-term trend was an accumulative loss with some resilience (Amani et al., 2022).

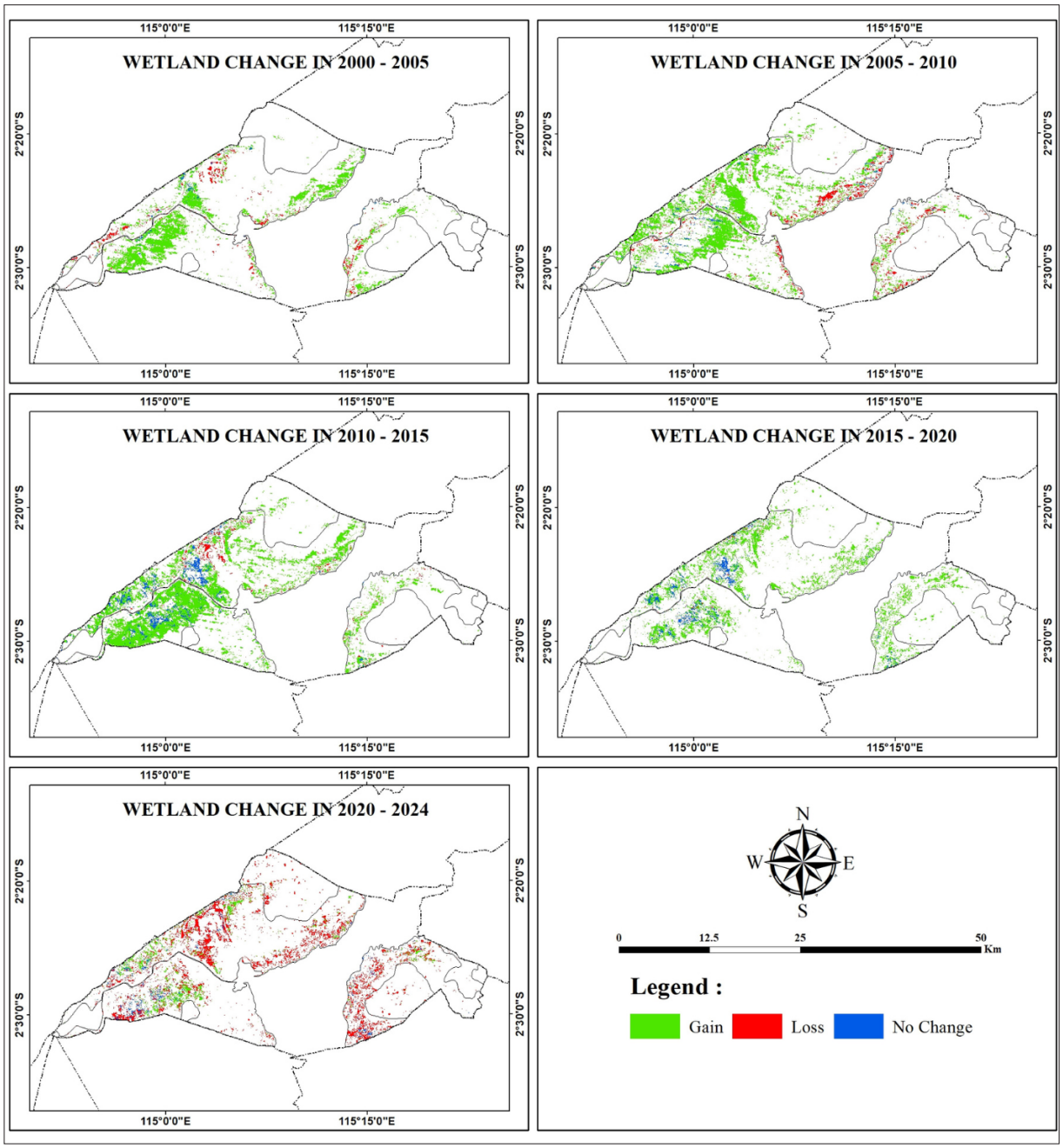

Figure 7. Wetland change and no change

3.5 Index Results

The dynamics of surface moisture and vegetative vigor surrounding the Hulu Sungai Utara wetland were illustrated by spectral water and vegetation indices derived from multitemporal satellite imagery between 2000 and 2024. Figure 8 shows the observed NDVI values from 2000 and 2024, with the lowest score being -0.69 and the highest being +0.87. Since the value of the NDVI parameter was less than zero, the red color signified no vegetation. Wetland was added between 2005 and 2010, specifically the larger water bodies. Due to the long dry season during that time, the wetland area was reduced between 2015 and 2020.

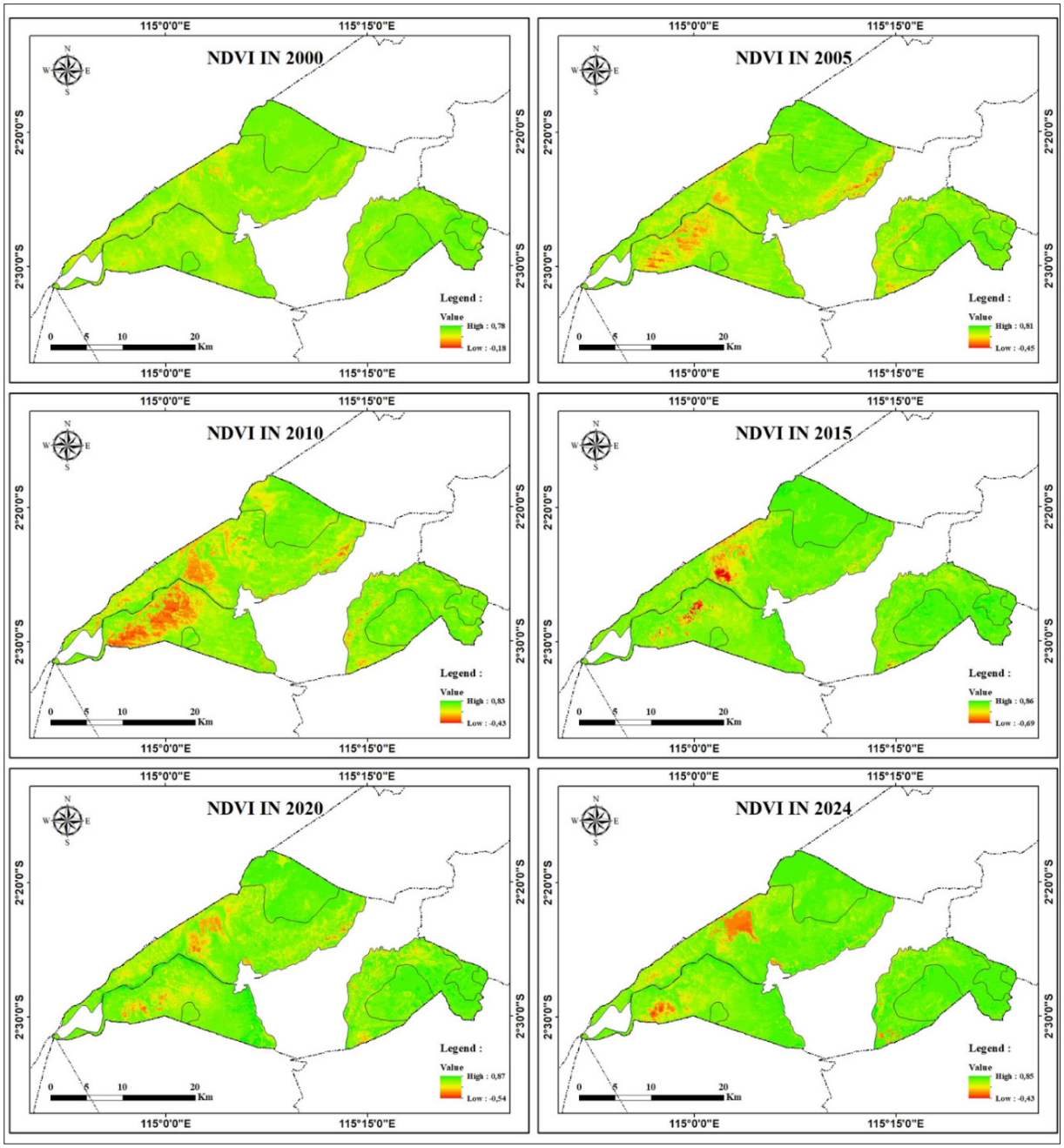

Figure 8. Result from NDVI

NDWI high-resolution satellite image data for the period from 2000 to 2024 was used to identify surface water bodies in the study area, as shown in Figure 9. During the analysis, the values ranged on average from -0.77 to +0.67. High plant water content and low vegetation content were represented by positive and negative NDWI values. Additionally, levels drop during the water stress phase, where low vegetation water content and vegetation fraction cover correlated with low NDWI results. NDVI values were greater than NDWI during the post-harvest wetland planting phase.

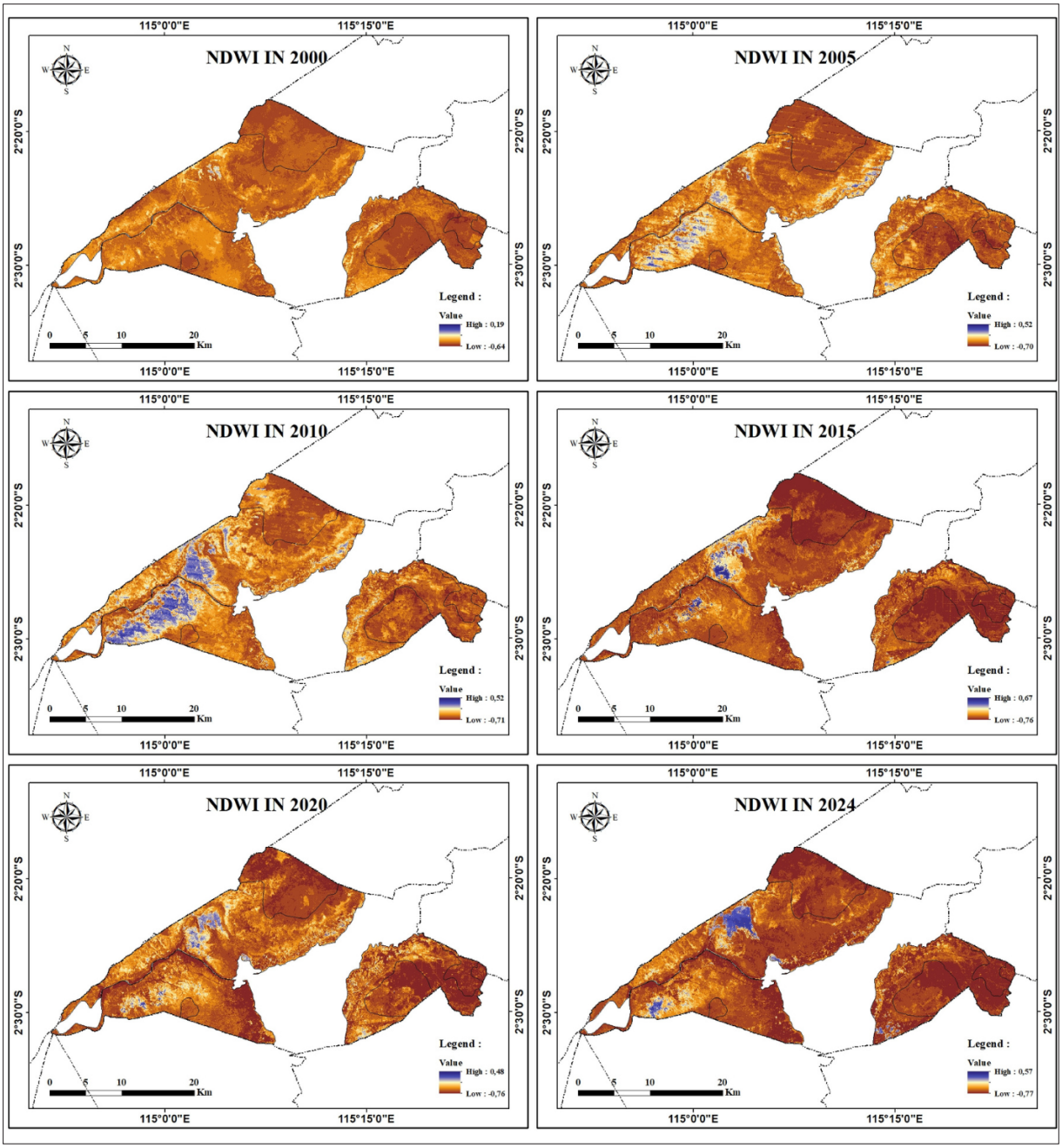

Figure 9. Result from NDWI

The surface water level decreased during the analysis period as observed from the decrease in the upper range of MNDWI values, which ranged from 0.62 in 2015 to 0.99 in 2005 and 2010 as shown in Figure 10. This result was consistent with the shrinkage observed in change studies of peatland regions. The lower limit of MNDWI decreased over time, signifying that even a slight loss of surface moisture occurred in some wetland areas (Ridwan et al.. 2022).

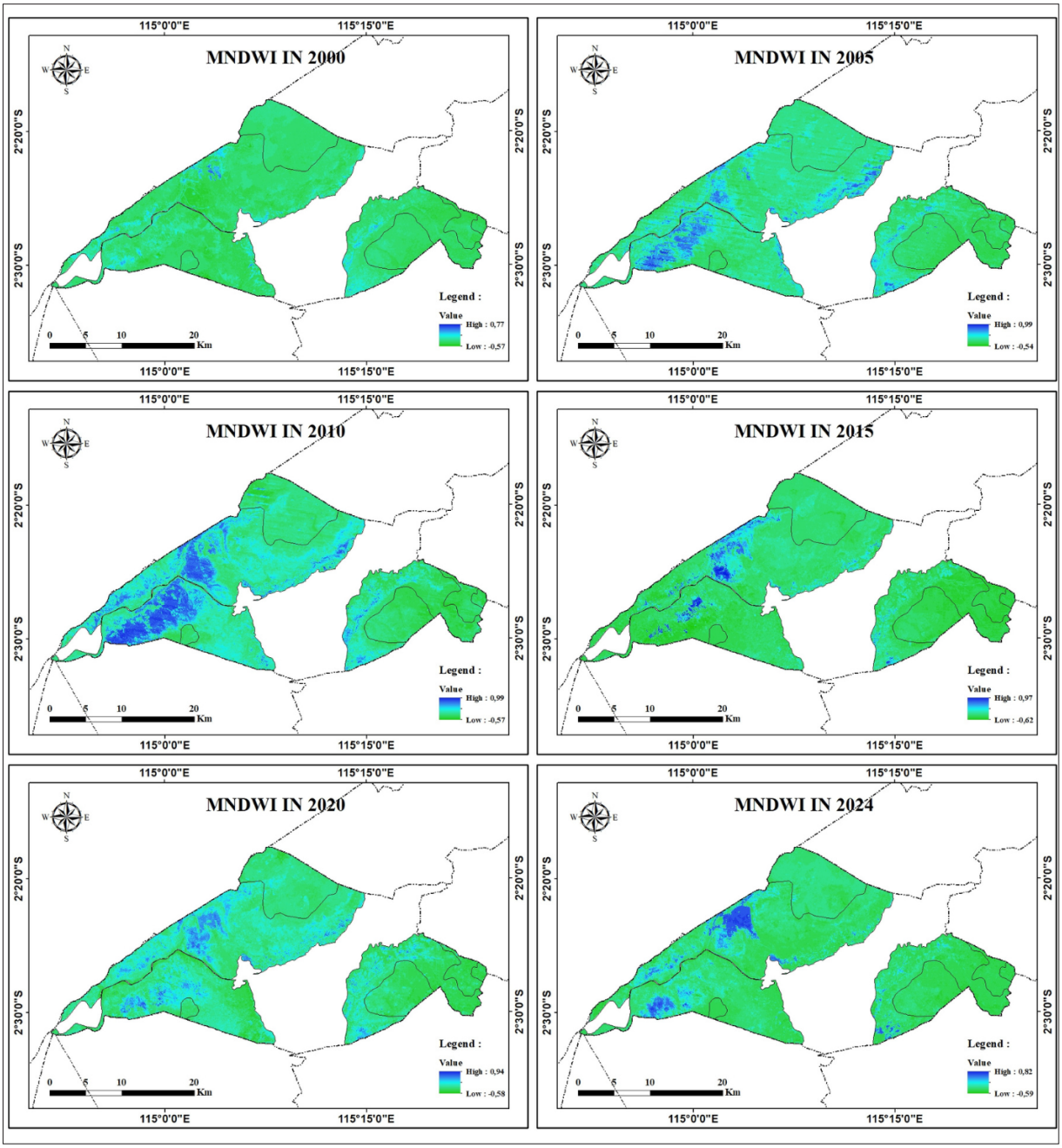

Figure 10. Result from MNDWI

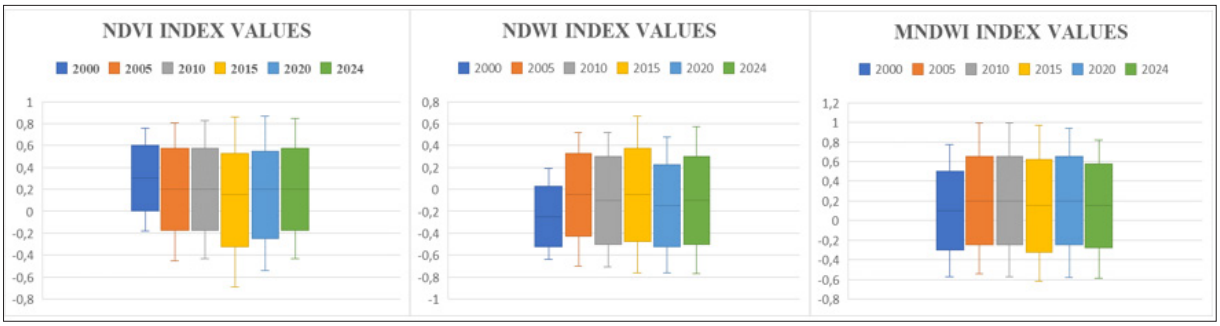

Figure 11. Distribution of NDVI, NDWI, and MNDWI index values for different years (2000, 2005, 2010, 2015, 2020, and 2024)

Figure 11 shows the distribution of NDVI, NDWI, and MNDWI index values for different years (2000, 2005, 2010, 2015, 2020, and 2024) in the study area. It is clear that the distribution and median values for each index (NDVI, NDWI, MNDWI) vary from year to year. This variation indicates changes in land cover conditions (vegetation, water) in the study area from 2000 to 2024. An increase in the median NDVI value or a higher scatter on the positive side tends to indicate an increase in vegetation cover or health in the study area. Conversely, a decrease in NDVI indicates

degradation of vegetation or land conversion (Jia et al., 2019). Higher values of these indices are generally associated with the presence of water or higher humidity. Changes in the median values and distribution of the MNDWI and NDWI from year to year may indicate fluctuations in the extent of waterlogging, soil moisture levels, or other hydrological changes in the wetland. A shift of the box towards more negative values could indicate a decrease in surface water availability or moisture. The NDVI is high, but the NDWI/MNDWI is low, indicating vegetated dry conditions, or vice versa, indicating waterlogging with vegetation less prominent in the image at the time of acquisition.

4. Conclusion

In conclusion, wetlands serve as essential ecosystems, providing natural resources, biological habitats, and ecological buffers. However, the land was also vulnerable to degradation as a result of overexploitation, infrastructure expansion, and climate change. The dynamic changes in wetland cover in Hulu Sungai Utara Regency from 2000 to 2024 were examined both temporally and spatially by applying NDVI, NDWI, and MNDWI indices along with machine learning methods, such as RF and SVM, using data from Landsat 7 and 8. During this analysis, RF performed better than other methods, achieving a total accuracy of 97.33% and an average kappa of 96%. Although the long-term trend still signified a total decline, the results showed a significant shift in wetlands, including greater regeneration than loss over the previous 15 years. The need for GEE-based geospatial technologies to aid data-driven decision-making in managing and protecting tropical wetland ecosystems is evident, as recent conservation initiatives are starting to have a positive impact.

Beyond summarizing changes, this study offers a key scientific contribution by providing a detailed, quantitative understanding of long-term wetland dynamics in Hulu Sungai Utara using a robust GEE-based approach that combines spectral indices and machine learning. It uniquely highlights a significant recent regeneration trend amidst overall decline, offering novel insights into ecosystem resilience and the effectiveness of conservation efforts The findings provide essential data and a framework for data-driven land-use planning, environmental management, and targeted conservation strategies, which are crucial for the sustainable future of these vital tropical wetlands.

Acknowledgments

The authors are grateful to the Ministry of Education, Culture, Study, and Technology for funding this study through the National Competitive Applied Study Grant [Number 056/E5/PG.02.00.PL/2024]. This support was instrumental in conducting and completing this study.

Authors Contribution

Conceptualization, N.N and I.R.; Methodology, N.N.; Software, I.R.; Validation, Y.F., N.N. and I.R.; Formal Analysis, Y.F.; Writing – Original Draft Preparation, Y.F.; Writing – Review & Editing, N.N.; Visualization, I.R.; Supervision, N.N.; Funding Acquisition, I.R.

Declaration Of Competing Interest

"The authors declare no conflict of interest."

References

Abdelmajeed. A. Y. A. Albert-Saiz M. Rastogi. A. & Juszczak. R. (2023). Cloud-Based Remote Sensing for Wetland Monitoring-A Review. In Remote Sensing (Vol. 15. Issue 6). MDPI. https://doi.org/10.3390/rs15061660

Amani. M. Kakooei. M. Ghorbanian. A. Warren. R. Mahdavi. S. Brisco. B. Moghimi. A. Bourgeau-Chavez. L. Toure. S. Paudel. A. Sulaiman. A. & Post. R. (2022). Forty Years of Wetland Status and Trends Analyses in the Great Lakes Using Landsat Archive Imagery and Google Earth Engine. Remote Sensing. 14(15). https://doi.org/10.3390/rs14153778

3. Aljanabi, F. K., & Dedeoğlu, M. (2025). Machine learning algorithms and geographic information system techniques to predict land suitability maps for wheat cultivation in the Central Anatolia Region. Journal of Ecological Engineering, 26(1), 373–387. https://doi.org/10.12911/22998993/196044

Andini, W. T., Nurlina, & Ridwan, I. (2024). Monitoring Vegetation Change Using Forest Cover Density Model. Ecological Engineering and Environmental Technology, 25(9), 369–378. https://doi.org/10.12912/27197050/190928

Awawdeh, M., Alkhateeb, E., & Al-Radaideh, N. (2023). The Use of Remote Sensing and GIS for Mapping Silica Sand Deposits in Jordan. Jordan Journal of Earth and Environmental Sciences, 14(3), 232–240.

Ashok. A. Rani. H. P. & Jayakumar. K. V. (2021). Monitoring of dynamic wetland changes using NDVI and NDWI based landsat imagery. Remote Sensing Applications: Society and Environment. 23. https://doi.org/10.1016/j.rsase.2021.100547

Aslam. R. W. Shu. H. Naz. I. Quddoos. A. Yaseen. A. Gulshad. K. & Alarifi. S. S. (2024). Machine Learning-Based Wetland Vulnerability Assessment in the Sindh Province Ramsar Site Using Remote Sensing Data. Remote Sensing. 16(5). https://doi.org/10.3390/rs16050928

DeLancey. E. R. Czekajlo. A. Boychuk. L. Gregory. F. Amani. M. Brisco. B. Kariyeva. J. & Hird. J. N. (2022). Creating a Detailed Wetland Inventory with Sentinel-2 Time-Series Data and Google Earth Engine in the Prairie Pothole Region of Canada. Remote Sensing. 14(14). https://doi.org/10.3390/rs14143401

Farda, N.M. (2017) 'Multi-temporal Land Use Mapping of Coastal Wetlands Area using Machine Learning in Google Earth 'Engine', IOP Conference Series: Earth and Environmental Science, 98(1). Available at: https://doi.org/10.1088/1755-1315/98/1/012042

Ghosh. S. Dasgupta. A. & Swetapadma. A. (2019). A Study on Support Vector Machine based Linear and Nonlinear Pattern Classification. In 2019 International Conference on Intelligent Sustainable Systems (ICISS).

Hashim. H. Abd Latif. Z. & Adnan. N. A. (2019). Urban Vegetation Classification With Ndvi Threshold Value Method With Very High Resolution (Vhr) Pleiades Imagery. International Archives of the Photogrammetry. Remote Sensing and Spatial Information Sciences - ISPRS Archives. 42(4/W16). 237–240. https://doi.org/10.5194/isprs-archives-XLII-4-W16-237-2019

Ichsan Ali. M. Darma Dirawan. G. Hafid Hasim. A. & Rais Abidin. M. (2019). Detection of Changes in Surface Water Bodies Urban Area with NDWI and MNDWI Methods. 9(3).

Jia, M., Wang, Z., Wang, C., Mao, D., & Zhang, Y. (2019). A new vegetation index to detect periodically submerged mangrove forest using single-tide Sentinel-2 imagery. Remote Sensing, 11(17), 1–17. https://doi.org/10.3390/rs11172043

Khalaf. A. B. (2024). Using Geospatial Techniques to Analysis the Impact of Climate Change on Water and Agriculture Resources: Case study Khanaqin District in Diyala. Iraq.

Basrah Journal of Agricultural Sciences. 37(1). 55–70.

https://doi.org/10.37077/25200860.2024.37.1.05

Laonamsai. J. Julphunthong. P. Saprathet. T. Kimmany. B. Ganchanasuragit. T. Chomcheawchan. P. & Tomun. N. (2023). Utilizing NDWI. MNDWI. SAVI. WRI. and AWEI for Estimating Erosion and Deposition in Ping River in Thailand. Hydrology. 10(3). https://doi.org/10.3390/hydrology10030070

Long, X. et al. (2021) 'Mapping the vegetation distribution and dynamics of a wetland using adaptive-stacking and Google Earth Engine based on multi-source remote sensing 'data', International Journal of Applied Earth Observation and Geoinformation, 102, p. 102453. Available at: https://doi.org/10.1016/j.jag.2021.102453

Ludwig. C. Walli. A. Schleicher. C. Weichselbaum. J. & Riffler. M. (2019). A highly automated algorithm for wetland detection using multi-temporal optical satellite data. Remote Sensing of Environment. 224. 333–351. https://doi.org/10.1016/j.rse.2019.01.017

Mahdavi. S. Salehi. B. Granger. J. Amani. M. Brisco. B. & Huang. W. (2018). Remote sensing for wetland classification: a comprehensive review. In GIScience and Remote Sensing (Vol. 55. Issue 5. pp. 623–658). Taylor and Francis Inc. https://doi.org/10.1080/15481603.2017.1419602

Mirmazloumi. S. M. Moghimi. A. Ranjgar. B. Mohseni. F. Ghorbanian. A. Ahmadi. S. A. Amani. M. & Brisco. B. (2021). Status and trends of wetland studies in Canada using remote sensing technology with a focus on wetland classification: A bibliographic analysis. Remote Sensing. 13(20). https://doi.org/10.3390/rs13204025

Mohammadi. M. Rashid. T. A. Karim. S. H. T. Aldalwie. A. H. M. Tho. Q. T. Bidaki. M. Rahmani. A. M. & Hosseinzadeh. M. (2021). A comprehensive survey and taxonomy of the SVM-based intrusion detection systems. In Journal of Network and Computer Applications (Vol. 178). Academic Press. https://doi.org/10.1016/j.jnca.2021.102983

Nedd. R. Light. K. Owens. M. James. N. Johnson. E. & Anandhi. A. (2021). A synthesis of land use/land cover studies: Definitions. classification systems. meta-studies. challenges and knowledge gaps on a global landscape. In Land (Vol. 10. Issue 9). MDPI. https://doi.org/10.3390/land10090994

Nurlina. Ridwan. I. Muslimin. S. & Roup. A. (2024). Peatlands changes analysis in Banjar District using three decades of Landsat imagery. Journal of Physics: Conference Series. 2866(1). https://doi.org/10.1088/1742-6596/2866/1/012073

Nurlina. Kadir. S. Kurnain. A. Ilham. W. & Ridwan. I. (2023). Impact of Land Cover Changing on Wetland Surface Temperature Based on Multitemporal Remote Sensing Data. Polish Journal of Environmental Studies. 32(3). 2281–2291. https://doi.org/10.15244/pjoes/157495

Rashid. M. B. (2023). Monitoring of drainage system and waterlogging area in the human-induced Ganges-Brahmaputra tidal delta plain of Bangladesh using MNDWI index. Heliyon. 9(6). https://doi.org/10.1016/j.heliyon.2023.e17412

Ridwan. I. Nurlina. & Putri. W. E. (2022). Estimation of Peatland Fire Carbon Emissions Using Remote Sensing and GIS Physics Study Program. Faculty of Mathematics and Natural Sciences Lambung Mangkurat. International Journal of Biosciences. 20(6). 246–253. http://dx.doi.org/10.12692/ijb/20.6.246-253

Shashikant. V. Shariff. A. R. M. Wayayok. A. Kamal. R. Lee. Y. P. & Takeuchi. W. (2021). Utilizing TVDI and NDWI to classify severity of agricultural drought in Chuping. Malaysia. Agronomy. 11(6). https://doi.org/10.3390/agronomy11061243

Sherstobitov. D. N. Ermakov. V. V. Bochkina. A. A. Tupitsyna. O. V. Bykov. D. E. & Chertes. K. L. (2021). Monitoring of the hydrological regime of the Saratov reservoir using the MNDWI index. IOP Conference Series: Earth and Environmental Science. 818(1). https://doi.org/10.1088/1755-1315/818/1/012048

Stehman. S. V. (1997). & Forestry. 320 Bray Hall. Syrxusr. NY 13210. In Remote Sens. Envihon (Vol. 62). OElsevier Science Inc.

Thanh Noi, P., & Kappas, M. (2017). Comparison of Random Forest, k-Nearest Neighbor, and Support Vector Machine Classifiers for Land Cover Classification Using Sentinel-2 Imagery. Sensors (Basel, Switzerland), 18(1). https://doi.org/10.3390/s18010018

Waleed, M. et al. (2023) 'Machine learning-based spatial-temporal assessment and change transition analysis of wetlands: An application of Google Earth Engine in Sylhet, Bangladesh (1985–2022)', Ecological Informatics, 75(March), p. 102075. Available at: https://doi.org/10.1016/j.ecoinf.2023.102075

Wu. L. Li. Z. Liu. X. Zhu. L. Tang. Y. Zhang. B. Xu. B. Liu. M. Meng. Y. & Liu. B. (2020). Multi-type forest change detection using BFAST and monthly landsat time series for monitoring spatiotemporal dynamics of forests in subtropical wetland. Remote Sensing. 12(2). https://doi.org/10.3390/rs12020341

Yan. X. Li. J. Yang. D. Li. J. Ma. T. Su. Y. Shao. J. & Zhang. R. (2022). A Random Forest Algorithm for Landsat Image Chromatic Aberration Restoration Based on GEE Cloud Platform—A Case Study of Yucatán Peninsula. Mexico. Remote Sensing. 14(20). https://doi.org/10.3390/rs14205154

Zhang. X. Liu. L. Zhao. T. Chen. X. Lin. S. Wang. J. Mi. J. & Liu. W. (2023). GWL-FCS30: a global 30m wetland map with a fine classification system using multi-sourced and time-series remote sensing imagery in 2020. Earth System Science Data. 15(1). 265–293. https://doi.org/10.5194/essd-15-265-2023

Zhu, Y. et al. (2024) 'Monitoring Land Use Changes in the Yellow River Delta Using Multi-Temporal Remote Sensing Data and Machine Learning from 2000 to '2020', pp. 1–18.